Flight Dynamics of Micro Air Vehicles with Morphing Horizontal-Tail Geometry

Adam Edstrand*
University of Florida, Gainesville, FL, 32611

As a bird is in flight, the tail feathers change geometry for different situations encountered during flight. The entire tail is a dynamic system that is dependent on active flight situations. This implicates that morphing the geometry of the horizontal-tail of an air vehicle would be beneficial to the flight dynamics. This paper considers eighteen different geometries of a micro air vehicle's horizontal-tail, varying the leading and trailing edge slope and the area while keeping the span of the tail fin constant. The concept of morphing geometries has been applied in micro air vehicles' wings to maintain yaw stability while rapidly pitching and rolling. Incorporating the ability to morph the tail fin as well may help improve the vehicle's effectiveness in flight.

Nomenclature

α	=	angle of attack
C_D	=	drag coefficient
C_L	=	lift coefficient
Λ	=	leading edge sweep
Γ	=	trailing edge sweep
Cm_α	=	rate of change of pitch moment with respect to angle of attack
Cm_{d2}	=	pitching moment with respect to changing elevator
CX_{d2}	=	elevator control effectiveness with respect to the force in the x direction
CZ_{d2}	=	elevator control effectiveness in the Z direction

I. Introduction

Modern aircrafts are designed to fit different purposes and design problems such as long range and efficiency, speed, maneuverability and other characteristics. The aerodynamic system, in most cases, is a static system which has minimal variation such as the cross-section geometry of the wing by use of slats and flaps. These systems are used to maximize lift and minimize drag by modifying the coefficients of lift and drag for the optimal in-flight condition. The evolution of the cross-section of an airfoil and the planform geometry of the wing has been modified over the history of flight.

Since the Wright brothers, aircrafts have been continually evolving. With the assistance of research, aerodynamics is understood more clearly and research in turn can be applied to more complex systems. Some of the systems that have been developing are Unmanned Air Vehicles (UAV) and Micro Air Vehicles (MAV) for application of moving in urban environments for surveillance, and improving targeting systems to name a few. Another more recent system that increases diversity of the flight dynamics of aircrafts is actively morphing the geometry of the aircraft's wing surfaces in-flight. Since flight dynamics are heavily dependent on the geometry, morphing the geometry in flight to a more optimal position could prove to be beneficial. The equations of motion prove to be void when asymmetric morphing occurs due to a change in aerodynamics and inertial changes which cause a violation of assumptions.[1] This paper will focus on the properties of MAV. MAV are UAV whose dimensional properties such as airspeed and span are smaller than traditional systems.[2]

Bionics, the study of biological methods and nature handles different tasks and engineering applicable problems, is a common process in which engineering and science problems are approached. Observing a bird in flight is an example of how to benefit from nature's evolution and adaptation. A bird flies by generating both thrust and lift

* Undergraduate Student; Department of Mechanical and Aerospace Engineering, *edstrand@ufl.edu*, Student Member AIAA

through the flapping of flexible wings. It has been found that in the forward thrust and efficiency of biological systems in a fluid is partially dependent on the geometry of the wings or fins.[3] The geometry of a bird's wing morphs into shapes that are dependent on whether it is gliding, diving or is in propelled flight. Taking this concept of morphing the wings of a MAV of similar size, the flight dynamics of the MAV changes as expected due to the change in geometry.

Morphing the wings of MAV to increase maneuverability has been done in practice by graduate students and is in their thesis papers.[1,4] Biological influence can be applied further by the astute observation that when a bird is in flight, its tail morphs as much as its wings. The morphing tail of birds implies that it is done to improve the flight dynamics for different situations encountered in flight. To take advantage of the capabilities of morphing the horizontal-tail of MAV, as was done in the above mentioned papers, an understanding of the changing geometries must be obtained. As with most engineering problems, the concept is first put to test in theory. This paper focuses on the flight dynamics of different geometries of the horizontal-tail. The collective data was obtained by the use of a program which develops the data by the numerical vortex panel method.

II. Methods

The Athena Vortex Lattice (AVL)[5] program, a computational program which was intended for aircraft aerodynamic and control analysis, was used in the research detailed below. For the formation plane in the program, a numerical approach was used by having sections of the main surfaces of the plane such as the wing, horizontal-tail, vertical-tail and so forth. The main input file in which the geometry was defined and configured had the suffix .avl. The geometry of the wing and vertical-tail was computed by previously generated computer models[6] and only the horizontal-tail was varied. Other optional files were used one which was denoted by the suffix .mass, which described the masses, inertias and dimensional units of the plane. The final optional input file used was denoted by the suffix .run and denoted all the run case input information of program including the velocity, bank angle, etc. The run cases could be altered after the program was executed by keystrokes by the user. Both the data within the .mass and .run files stayed constant throughout the cases in this paper. The prefix of these files must share an arbitrary name, which in this paper reflected the case number.

In each case performed, only the horizontal-tail's geometry was modified while the span of the horizontal-tail was held constant. Elementary algebra was used in finding the slope and chord lengths of the horizontal-tail and the work will be omitted in the interest of space. The horizontal-tail initially was held as a swept V. In the first four cases, while keeping the leading edge sweep angle, Λ, and the chord length of the outer most edge constant, the trailing edge was morphed by increasing the middle of the horizontal-tail's chord length by .5 units until the geometry became a delta shaped horizontal-tail.

In the fourth through ninth case, the trailing edge of the horizontal-tail was kept at an angle of 0°, or as a straight line, and the sweep angle was decreased until it also had an angle of 0°, creating a square horizontal-tail configuration of chord length 3.5 units.

For the latter nine cases, the horizontal-tail was morphed oppositely of the former nine cases. That is, for the first five cases, the leading edge stayed constant with a sweep angle of 0° and the trailing edge's slope morphed until it was a reverse delta configuration, similar to case 4, which was normal delta style geometry. In the final four cases, the leading edge was morphed from a sweep angle of 0° to a reverse swept V geometry.

After the cases were created, the data were then obtained by running the program using MATLAB (The Mathworks, Natick, MA). When the program was executed, the plane was constructed using the .avl and .mass files while the run case was computed using the .run file. The AVL program offered two cases; case 1 which set the plane at level or banked horizontal flight constraints and case 2, which allows steady pitch, or looping, flight constraints. Case 1 was used and the constraints were given. The sideslip angle, β, was assumed to be 0° for all cases. The ailerons, elevators and rudder were calculated and held so that the roll moment, pitch moment and yaw moment were 0, respectively.

Once the constraints were entered, the run case was then executed and the program used the numerical vortex panel method to determine the required data necessary to stay within the given constraints. If more than 20 iterations were necessary to maintain the constraints given by the .run file, it was assumed that there was no solution and the program produced a trim convergence error. Once the run case was executed, the stability derivatives and body-axis derivatives were obtained and the data were recorded. This process was done for each run case and the data were compiled.

III. Influences and Modeling of the MAV

A. Natural Correlation

Over the course of millions of years, nature has solved many problems encountered by modern day scientists and engineers through adaptation, natural selection and other evolutionary processes. Bionics can be utilized to improve modern day engineering problems. Humans have learned to benefit from observing and replicating traits found in nature in many fields outside the science and engineering field. Engineers and scientists can learn from nature to not only solve current engineering problems but to improve previously solved problems.

Comparing birds and planes in flight, the first thing noticed from a geometric standpoint is the lack of a vertical-tail in birds. Research has been done on how birds maintain yaw stability without a vertical-tail to act as a rudder. It was stated that by varying the wings and the tail's geometry, yaw stability is maintained due to a morphing in the lateral direction. It was also notable that birds with wings that have slotted tips help maintain yaw stability when a sideslip moment is created.[7,8] In this paper, yaw stability was made obsolete by setting β equal to 0° so that the relative wind of the airplane was straight forward and no yawing moments were produced. Studying flight characteristics and dynamics of birds further could prove beneficial in the design of aircrafts without the need of vertical-tails.

B. Modern Aircraft Characteristics

Modern aircrafts have wide varieties of geometries from delta shaped wings to swept V's to forward swept wings, all for different purposes. Wing sweep is a large factor in an aircraft wing's planform design, having the largest effect on lift and drag due to the normal component of the relative airflow on the leading edge of the wing. Transonic aircrafts which have swept wings have less drag with increased stability and control characteristics.[9] Delta and forward swept wings are common among experimental aircraft and was an interest to be studied as well.

In this paper, the concepts of a wing's geometry were translated to the horizontal-tail and the flight dynamics were analyzed. The horizontal-tail changes design for different aircrafts as the wings do. The geometry of many commercial airliners' airplanes is a swept configuration, whereas many of the military's aircraft geometries are closer to a delta configuration. Some experimental aircrafts, such as the Grumman X-29, move the horizontal-tail aft of the main lifting surfaces as canard control surface. This illustrates that horizontal-tail geometry varies for different aircrafts and that different geometries contribute differently to the flight dynamics of aircrafts.

C. Aircraft Model

The overall aircraft design including the body, planform and vertical-tail was borrowed from the a previously designed and built MAV, which can be seen in Figure 1, which has been designed, tested, and flown. The AVL coding and design has been used previously[6] and the mass and geometries were kept constant while modifying the horizontal-tail. In this paper steady flight conditions were considered and β was kept at 0°. The horizontal-tail's leading and trailing edge's geometry was morphed and the span was kept constant. Table 1 shows the angles between the y-axis, pointing out the right wing, and the leading and trailing edge for each case. This paper follows conventional sweep angles in which a positive sweep corresponds with horizontal-tail sweeping aft away from the nose of the air vehicle and a negative sweep corresponds with the horizontal-tail sweeping forward towards the nose of the air vehicle.

Figure 1. The original MAV design before the horizontal-tail was modified.

The eighteen cases could be grouped into four subgroups: case 1-4 where the leading edge was held constant and the trailing edge slope decreased to zero; case 5-9 where the trailing edge was held constant at zero and the sweep angle decreased to zero; case 10-14 where the leading edge was held constant at zero and the trailing edge decreased to a mirror image of case 4; and case 15-18 where the trailing edge was held constant and the leading edge decreased into a forward swept V. These are denoted subgroups 1-4, respectively. The overall MAV and the initial horizontal-tail position as well as the transformation between these four subgroups can be observed in Figure 2.

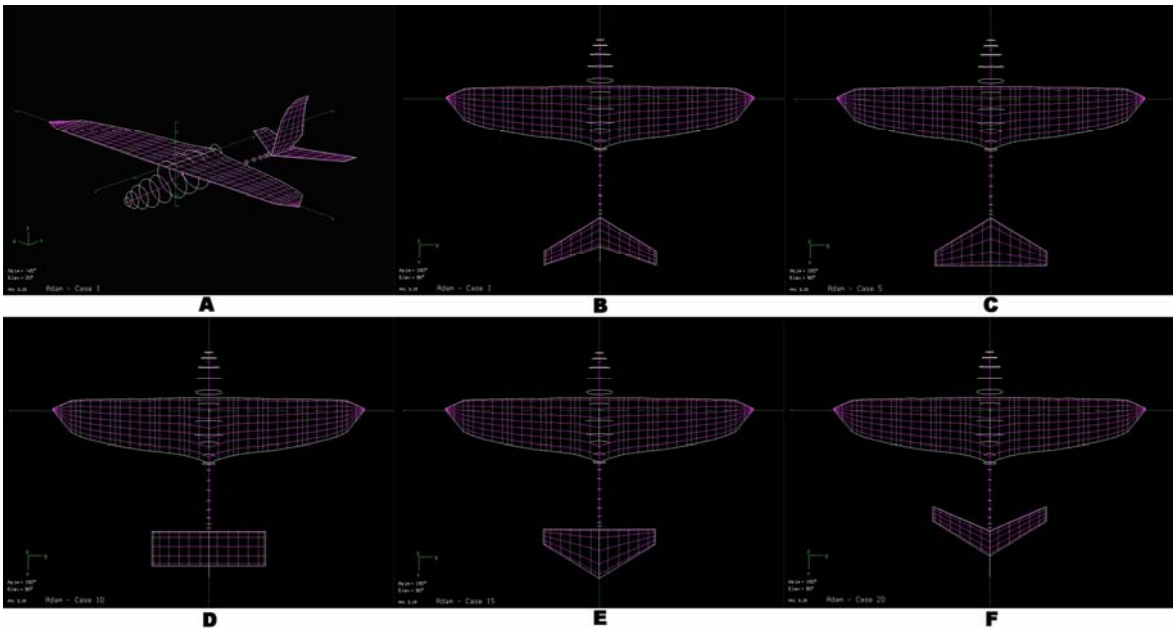

Figure 2. Subgroups of Cases. *A) Overall View of the MAV, B) Case 1 of the MAV prior to morphing any geometry, C) Case 5 of the MAV after morphing the trailing edge to 0°, D) Case 10 of the MAV after morphing the leading edge to 0°, E) Case 15 of the MAV after morphing the trailing edge to -31.4°, F) Case 20 of the MAV after morphing the leading edge to -23.5°.*

IV. Results and Discussion

A. Angle of Attack and Drag

The first piece of data observed when the data was compiled were the angle of attack, α, the coefficient of lift, C_L, and the coefficient of drag, C_D. C_L was constant throughout the paper because it was determined by velocity and α. C_L was constant because the velocity was constant throughout this paper and α was varied to keep a constant C_L, therefore it will not be discussed beyond this. It is worth noting that the plotted figures in this paper were done by grouping the data in which the leading edge was morphed while the trailing edge was constant (subgroup 2 and 4) and where the trailing edge was morphed and the leading edge was held constant (subgroup 1 and 3).

Table 1

Case Number	Leading- Edge Sweep, Λ, °	Trailing-Edge Sweep, Γ, °
Case 1	31.4	19.2
Case 2	31.4	9.9
Case 3	31.4	5.0
Case 4	31.4	0.0
Case 5	26.6	0.0
Case 6	18.4	0.0
Case 7	14.1	0.0
Case 8	11.3	0.0
Case 9	0.0	0.0
Case 10	0.0	-11.3
Case 11	0.0	-14.1
Case 12	0.0	-18.4
Case 13	0.0	-26.6
Case 14	0.0	-31.4
Case 15	-5.0	-31.4
Case 16	-9.9	-31.4
Case 17	-19.2	-31.4
Case 18	-23.5	-31.4

The C_D proved to be dependent on both the leading edge sweep angle, Λ, and the trailing edge angle, Γ. The trend was more obvious and continuous when Λ changed rather than Γ shown in Figure 3. It was quite apparent that when Λ decreased, C_D increased. In the cases in which Λ was constant and Γ was varying, the C_D was lowest when Γ was 0°. C_D was lower when Γ was positive, rather than when Γ was negative. This is illustrated in Fig. 4. These trends show that when Λ decreased and the leading edge morphed towards the relative wind and drag was induced; whereas if Γ was positive and the surface was moving with the relative wind, C_D will be lower than if Γ was negative and moving into the relative wind. This shows that for optimal drag reduction, the delta formation which had a steeper positive Λ would be best to employed. This was confirmed by noticing that case 4, which had the said delta configuration, had the lowest C_D.

The angle of attack helps produce lift in situations where lift is insufficient when α is 0°. The trade off of an increased angle of attack was that with the increased lift, there is also an increased drag. When α was plotted versus Λ and Γ, plots that were almost identical to the C_D plots versus Λ and Γ. This can be seen when comparing Figures 3 and 4 with Figures 5 and 6, respectively. This shows the direct correlation to drag and α which could be due to the flow separation behind the airfoil as α was increased causing a wake. This wake could have produced pressure drag which increased the overall drag of the air vehicle. This overall increase in drag was seen in the increase in C_D. This reinforced the previous statement that case 4 was the optimal case for minimal drag conditions because in case 4, α was at its minimum.

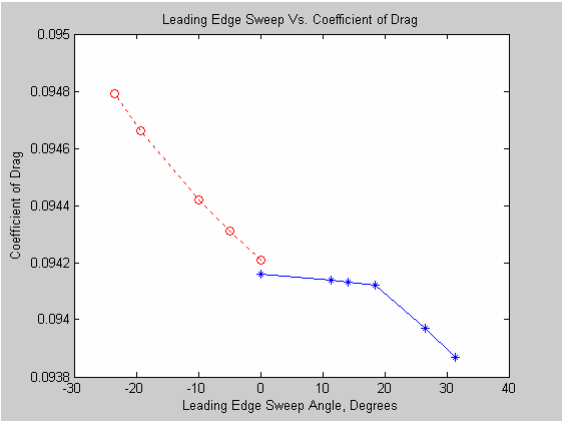

Figure 3. *Subgroup 2 which the leading edge was between 0° and 31.4° (blue -), Subgroup 4 which the trailing edge was between 0° and -23.5° (red --).*

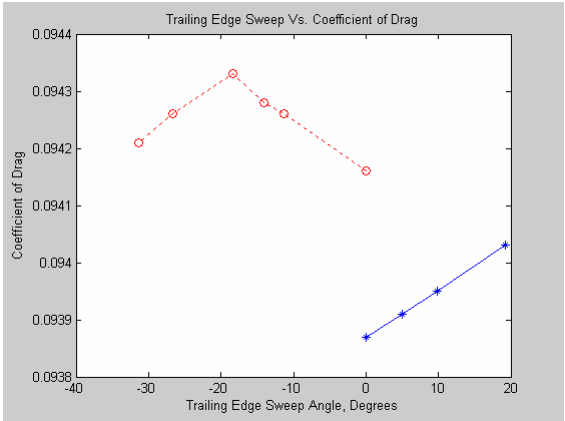

Figure 4. *Subgroup 1 which the trailing edge was between 0° and 19.2° (blue -), Subgroup 3 which the trailing edge was between 0° and -31.4° (red --).*

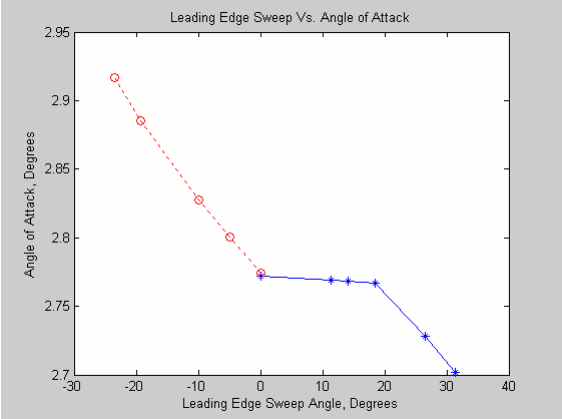

Figure 5. *Subgroup 2 which leading edge was between 0° and 31.4° (blue -), Subgroup 4 which the trailing edge was between 0° and -23.5° (red --). Note the similarities with Fig. 3.*

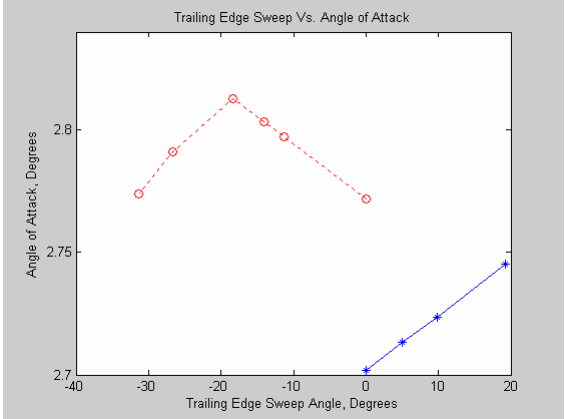

Figure 6. *Subgroup 1 which the trailing edge was between 0° and 19.2° (blue -), Subgroup 3 which the trailing edge was between 0° and -31.4° (red --). Note the similarities with Fig. 4.*

B. Elevator Deflection, and Stability Derivatives

The computer model was exposed to forward steady flight with which the roll moment, pitch moment and yaw moment would stay constant at 0. The program, when executed, would find the elevator deflection angle which kept the pitching moment at 0. The elevator deflected in a way which showed correlation with the C_D. As the elevator increased in angle away from the horizontal, Figure 3 and Figure 4 show an increase in C_D. This further reinforced the fact that when Γ was 0°, there was less drag and for conditions in which drag should be reduced, it was optimal to have Γ be 0°. When looking at the leading edge, the elevator deflection decreased in angle from the horizontal as Λ approached 0°. This actually showed that for a minimal deflection angle, the square horizontal-tail orientation was slightly more optimal than the delta configuration with a difference of .06°; a minute difference.

The stability of flight is as important as the L/D ratio because it incorporates dynamic situations such as wind gusts and other variables which may vary flight conditions. The rate of change of pitch moment with respect to the angle of attack, or Cm_α is a stability derivative which will be of interest in this paper because it has to do with the stability and how it changes with the change in geometry of the horizontal-tail. Other stability derivatives will be observed, including Cl_β and Cn_β, which should not change because they correspond with the roll and yaw stability of the aircraft and the horizontal-tail generally does not have much influence on those control factors.

Cm_α is ideally a large and negative number for stable aircraft. When a wind gust causes the aircraft's nose to pitch up, a negative Cm_α causes a moment that pitches the nose of the aircraft down, creating a statically stable condition. If Cm_α were positive, it would cause a moment which pitches the nose up further, causing static instability in the plane. In Figure 9 and Figure 10, it was illustrated that Cm_α had the highest negative value when Γ was equal to 0° and Λ was equal to 31.4°. This shows that the most stable pitching case was the case 4 configuration of delta horizontal-tail geometry with a Cm_α of -1.56. It should be noted that though this may be the most stable configuration, all of the cases were stable at least to a degree, where case 18 had the least amount of pitch stability. When comparing Cm_α in Figure 9 and Figure 10 to the elevator deflection plot in Figure 7 and Figure 8, it can be noticed that the Cm_α was similar to the negative of the elevator deflection plot. This implies that as the elevator deflection decreased, the negative value of Cm_α increased, therefore it made the aircraft more statically stable respective to the pitching axis.

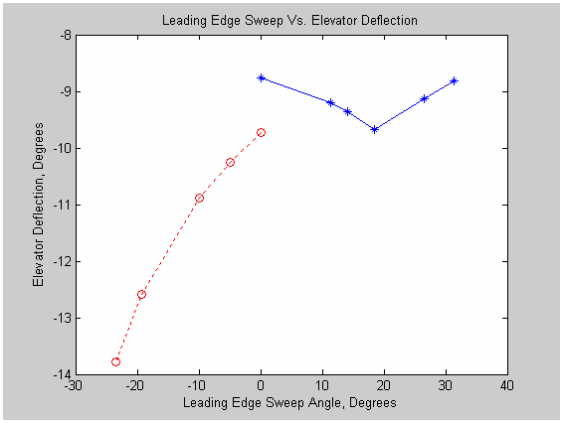

Figure 7. *Subgroup 2 which leading edge was between 0° and 31.4° (blue -), Subgroup 4 which the trailing edge was between 0° and -23.5° (red - -).*

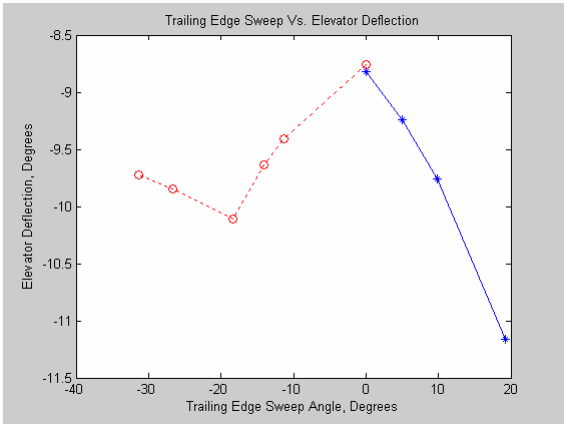

Figure 8. *Subgroup 1 which the trailing edge was between 0° and 19.2° (blue -), Subgroup 3 which the trailing edge was between 0° and -31.4° (red - -).*

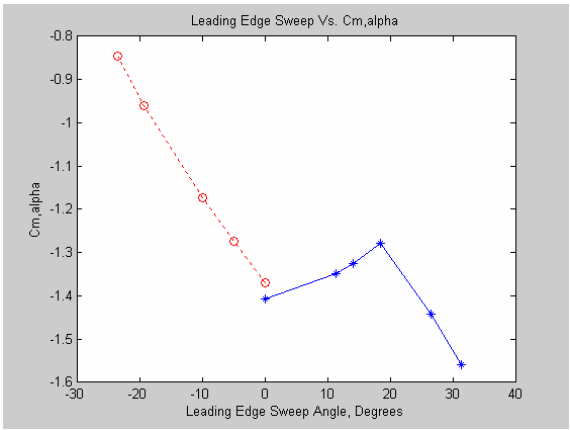

Figure 9. *Subgroup 2 which leading edge was between 0° and 31.4° (blue -), Subgroup 4 which the leading edge was between 0° and -23.5° (red - -).*

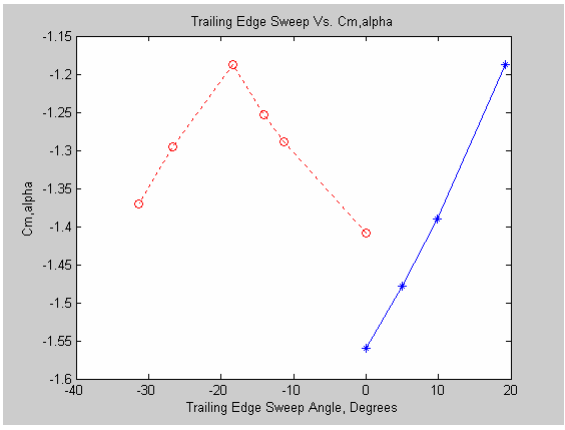

Figure 10. *Subgroup 1 which the trailing edge was between 0° and 19.2° (blue -), Subgroup 3 which the trailing edge was between 0° and -31.4° (red - -).*

The two stability derivatives Cn_β and Cl_β should have relatively small amounts of change with respect to Cm_α because the control surface being morphed was the horizontal-tail, which impacts the pitching moment more than the Cl_β's and Cn_β's respective roll and yaw moment. Since the surfaces that dealt directly with these two rates were held constant, the change of these values should be relatively small. This was confirmed when the difference between the maximum and minimum was taken, which displayed the differences for Cl_β and Cn_β were .0023 and .0042, respectively. Comparing to Cm_α's difference between maximum and minimum of .71, it was two orders of magnitude larger than Cl_β and Cn_β. This confirmed what was expected of the data.

When comparing the Cn_β plot, Figure 11 and 12, with the elevator deflection plot (Figure 7 and 8), there appeared to be a correlation between the two plots. This implied that Cn_β and the elevator deflection were related in some way. Figure 14 made it apparent that when the trailing edge changed sweep angle, the Cl_β plot was relatively unchanged compared to the leading edge sweep in Figure 13. This showed that for the relatively small change in Cl_β was mainly dependent on the change in Λ rather than Γ.

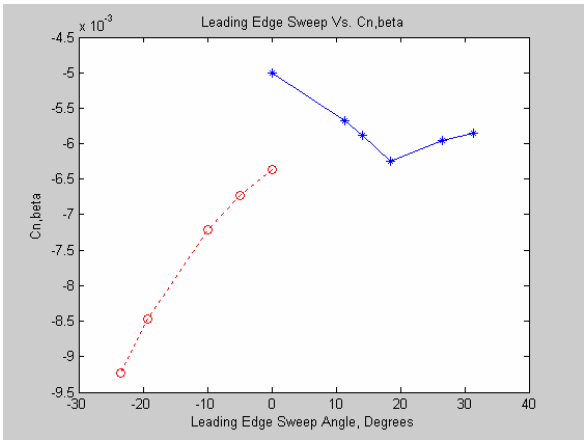

Figure 11. *Subgroup 2 which leading edge was between 0° and 31.4° (blue -), Subgroup 4 which the leading edge was between 0° and -23.5° (red - -).*

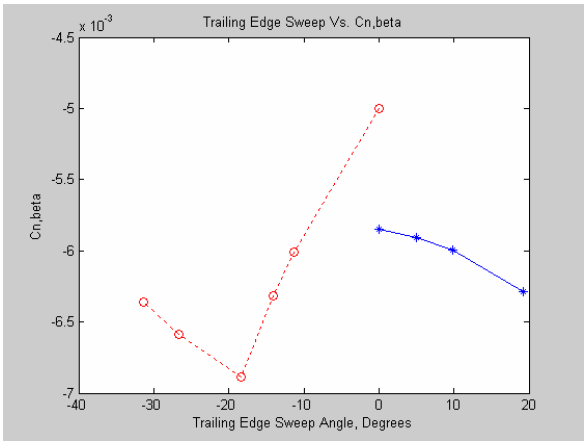

Figure 12. *Subgroup 1 which the trailing edge was between 0° and 19.2° (blue -), Subgroup 3 which the trailing edge was between 0° and -31.4° (red - -).*

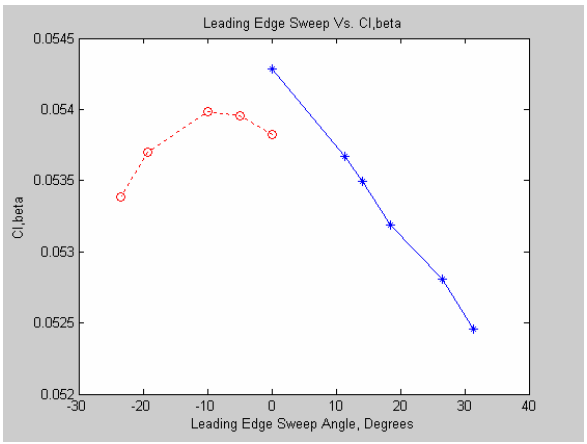

Figure 13. *Subgroup 2 which leading edge was between 0° and 31.4° (blue -), Subgroup 4 which the leading edge was between 0° and -23.5° (red - -).*

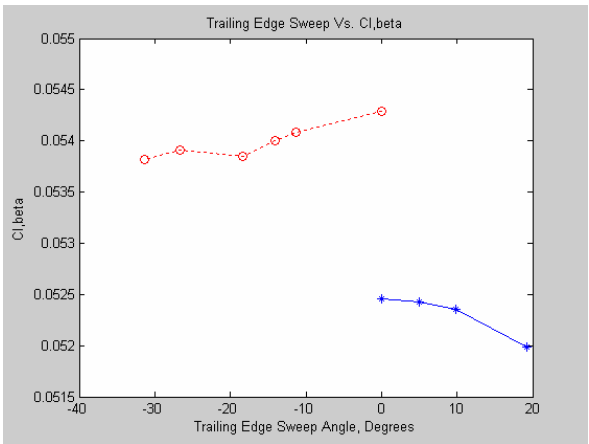

Figure 14. *Subgroup 1 which the trailing edge was between 0° and 19.2° (blue -), Subgroup 3 which the trailing edge was between 0° and -31.4° (red - -).*

C. Control Derivatives

Control derivatives have to do with the effectiveness of the control surfaces of the aircraft. There are different derivatives for each control surface including the aileron, elevator and rudder and were denoted by the subscript δ1, δ2 and δ3, respectively. For this paper, the elevator control derivatives will be considered because they are directly related to the horizontal-tail. $Cm_{\delta 2}$ is the control derivative with respect to the pitching moment whereas $CX_{\delta 2}$ and $CZ_{\delta 2}$ are the control derivative with respect to drag and lift, respectively. $Cm_{\delta 2}$ deals with the effectiveness of the

elevator in creating the pitching moment. The larger the number is, the more effective the elevator is on the pitching moment. In this paper, the sign was negative because of the coordinate system used in the paper.

When looking at Figure 15, it became clear that when Λ was negative, the $Cm_{\delta 2}$ became less effective at a linear rate, having a smaller negative number than any other cases. The two optimal cases were when the leading edge sweep was 0° and 31.4°; the latter being slightly more optimal. As the trailing edge became more positive, the effectiveness declined linearly as seen in Figure 16; meaning that as the aircraft has a higher positive Γ, the effectiveness of the elevator decreases. As Γ increased negatively, the effectiveness went down until Γ was 19.2°, then the effectiveness improved slightly. The optimal case of the trailing edge was when Γ was 0°. This shows that the delta configuration or square configuration, cases 4 and 9, respectively, had the most effective elevator.

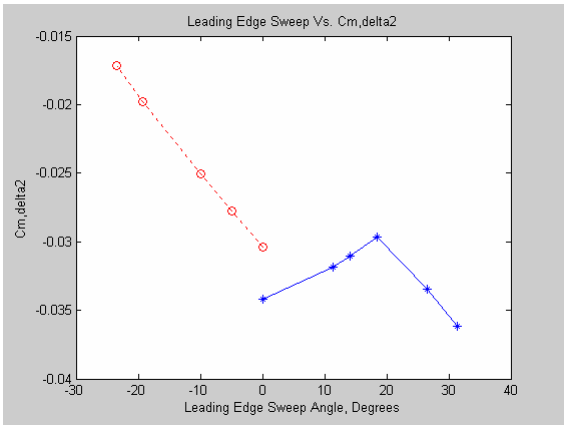

Figure 15. *Subgroup 2 which leading edge was between 0° and 31.4° (blue -), Subgroup 4 which the leading edge was between 0° and -23.5° (red - -).*

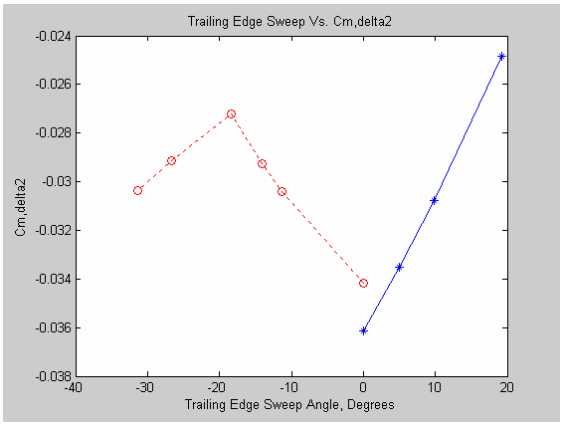

Figure 16. *Subgroup 1 which the trailing edge was between 0° and 19.2° (blue -), Subgroup 3 which the trailing edge was between 0° and -31.4° (red - -).*

Figure 17-20 involved the leading and trailing edge of $CX_{\delta 2}$ and the leading and trailing edge of $CZ_{\delta 2}$, respectively. $CX_{\delta 2}$ deals with the force in the x-direction, which corresponds with the drag on the model due to the elevator; whereas $CZ_{\delta 2}$ deals with the force in the z-direction, which corresponds with the lift on the model due to the elevator. Due to the design of an aircraft, it becomes apparent that $CZ_{\delta 2}$ should be significantly larger than $CX_{\delta 2}$ because it is ideal for the lift to drag ratio to be much larger than 1. This was illustrated in the aforementioned figures by noting that the values for $CX_{\delta 2}$ had a multiplier of 10^{-4}, which made them 1 order of magnitude smaller than $CZ_{\delta 2}$. Other than the multiplier, the subgroups had similar plots, meaning $CX_{\delta 2}$ and $CZ_{\delta 2}$ changed similarly. As Λ increased negatively, $CX_{\delta 2}$ and $CZ_{\delta 2}$ decreased linearly. This meant that the drag and lift both went down at similar rates.

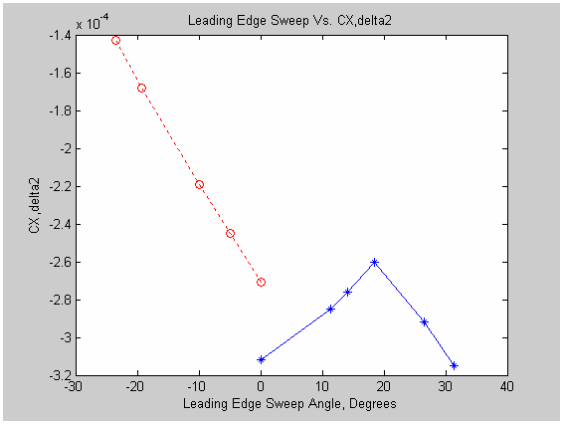

Figure 17. *Subgroup 2 which leading edge was between 0° and 31.4° (blue -), Subgroup 4 which the leading edge was between 0° and -23.5° (red - -).*

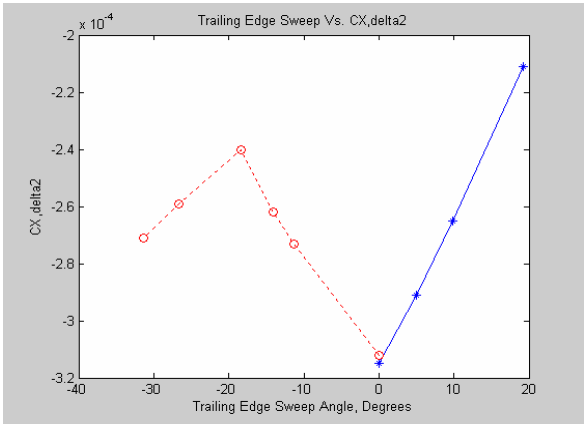

Figure 18. *Subgroup 1 which the trailing edge was between 0° and 19.2° (blue -), Subgroup 3 which the trailing edge was between 0° and -31.4° (red - -).*

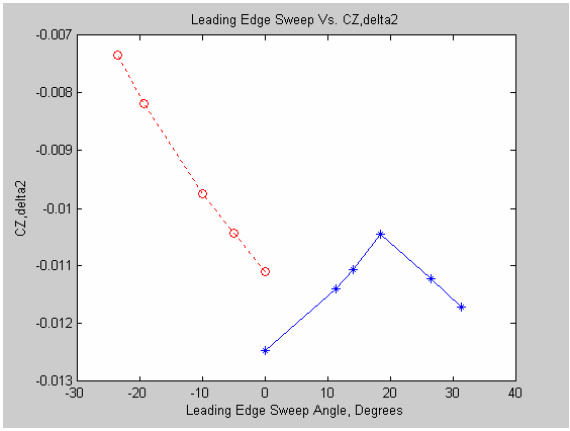

Figure 19. *Subgroup 2 which leading edge was between 0° and 31.4° (blue -), Subgroup 4 which the leading edge was between 0° and -23.5° (red - -).*

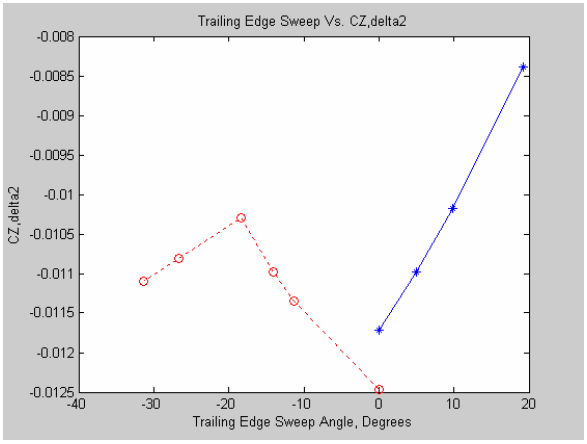

Figure 20. *Subgroup 1 which the trailing edge was between 0° and 19.2° (blue -), Subgroup 3 which the trailing edge was between 0° and -31.4° (red - -).*

In Figures 21 and 22, the ratio of $CZ_{\delta 2}$ over $CX_{\delta 2}$ was plotted with respect to the leading and trailing edge, respectively. This was used to estimate the lift to drag ratio for each case. The highest lift to drag ratio was 51.3 in case 18 with the forward swept model and the lowest for case 4 with the delta shaped model. This was counterintuitive because as shown in Figures 3 and 4, case 18 was actually the worst case for drag, whereas case 4 was the optimal case. This meant there was a higher increase in lift with case 18 than a decrease in drag. This case would be optimal when a higher lift to drag ratio is needed. It is worthy to note that case 18 was also the most unstable case so the instability should be weighed in with the decision before being considered the optimal case.

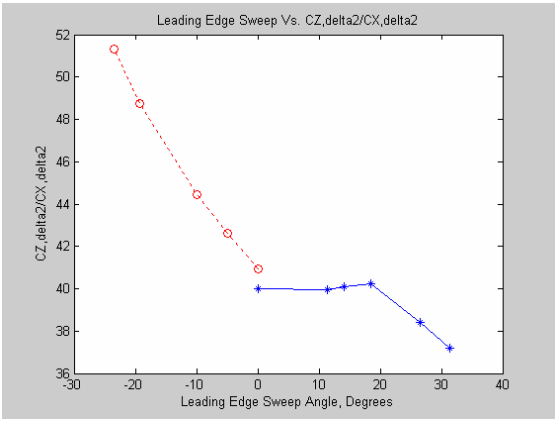

Figure 21. *Subgroup 2 which leading edge was between 0° and 31.4° (blue -), Subgroup 4 which the leading edge was between 0° and -23.5° (red - -).*

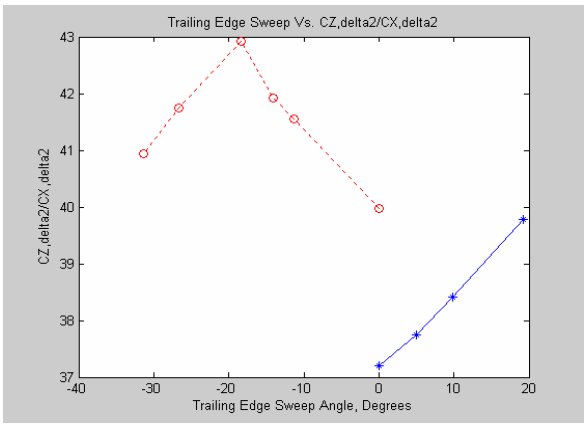

Figure 22. *Subgroup 1 which the trailing edge was between 0° and 19.2° (blue -), Subgroup 3 which the trailing edge was between 0° and -31.4° (red - -).*

V. Conclusion

Since the beginning of flight, aircrafts have progressed from static wings with no in-flight modification to including slats and flaps to slightly morph the wing's cross-section to optimize the aerodynamic efficiency. The future could entail actively morphing entire geometries of the wing to optimize the necessary in-flight condition. Morphing geometric properties of airplane in steady flight conditions to determine the aerodynamics, static stability and control efficiencies is one way to determine the optimal condition for different situations of flight. Micro Air Vehicles could be looked at as a prototype to larger scale models.

In this paper, different conditions were considered to produce optimal geometric positions. For the MAV in a situation which requires a large lift to drag ratio, it was found that the forwards swept geometry, case 18, was optimal, shown in Figure 21. It should also be observed that the stability of this case was the worst compared to other cases. This case was when the leading edge and trailing edge sweep angles were the largest in the negative

direction. This would be optimal when drag is not as large of an issue as lift, including take-off. When drag was the principal factor to be optimized, it would be conducive to have the leading edge at the largest positive sweep angle and the trailing edge at 0°, or in the delta formation of case 4. In this case the coefficient of drag was the smallest of all the cases and would be optimal in a situation such as cruising in steady flight for a long period of time. In the situation in which a large amount of pitch stability was necessary and Cm_{α} was a large negative value, when the leading edge was its largest positive value and the trailing edge was 0°. This, like drag, would be optimal when cruising in steady flight incase of in-flight situations such as wind gusts. When a large amount of control effectiveness, or negative $Cm_{\delta 2}$, is required, the optimal case would be case 4, where the leading edge is largest and the trailing edge is 0°. This would be optimal in a situation in which the Micro Air Vehicle would need to perform a maneuver which requires a large pitching moment.

This paper showed optimal geometric orientation for steady and static flight conditions. This paper did not consider dynamic flight conditions and the geometries were not geometries which would be easily morphed from one to another. For example, the situation which would need to morph from case 1 to case 18 or visa versa would be a difficult engineering problem to solve. Future studies would include asymmetric morphing and the flight dynamics involved. Overall, the optimal case for steady flight would be case 4 which is the delta configuration seen in Figure 2c. This case had the lowest C_D and the highest negative Cm_{α} which would give the highest fuel efficiency and highest stability of all the cases in the paper.

Acknowledgments

The author gratefully acknowledges Dr. Rick Lind for his support and the time spent teaching the author the stability and controls necessary to write this paper. Additionally, the author would like to thank Brian Roberts for the time it took to patiently explain the AVL program and code. Finally, the author would like to thank Dan Grant for selflessly supplying the code for the MAV examined in this paper.

References

[1] Abdulrahim, M., "Dynamic Characteristics of Morphing Micro Air Vehicles," Masters of Science Thesis, Department of Mechanical and Aerospace Engineering, University of Florida, Gainesville, FL 2004.

[2] Abdulrahim, M., Garcia, H., and Lind, R., "Flight Characteristics of Shaping the Membrane Wing of a Micro Air Vehicle," *Journal of Aircraft*, Vol. 42, No. 1, 2005, pp. 131 -137.

[3] Combes, S. A., and Daniel, T. L., "Shape, Flapping, and Flexion: Wing and Fin Design for Forward Flight," *The Journal of Experimental Biology*, 2001, 204: 2073-2085.

[4] Garcia, H., "Control of Micro Air Vehicles Using Wing Morphing," Masters of Science Thesis, Department of Mechanical and Aerospace Engineering, University of Florida, Gainesville, FL 2003.

[5] Drela, M. and Youngren, H., \AVL - Aerodynamic Analysis, Trim Calculation, Dynamic Stability Analysis, Aircraft Configuration Development," Athena Vortex Lattice, v. 3.15, http://raphael.mit.edu/avl/.

[6] Roberts, B., "Flight Dynamics of a Paleo-Inspired Aircraft Featuring a Variable-Placement Vertical Tail Design," to be published.

[7] Sachs, G., "Tail Effects on Yaw Stability in Birds," *Journal of Theoretical Biology*, 2007, 249: 464-472.

[8] Sachs, G., "Why Birds and Miniscale Airplanes Need No Vertical Tail," *Journal of Aircraft*, Vol. 44, No. 4, 2007, pp. 1159-1167.9

[9] Siouris, S. and Qin, N., "Study of the Effects of Wing Sweep on the Aerodynamic Performance of a Blended Wing Body Aircraft," *Proceedings of the Institute of Mechanical Engineers; Part G; Journal of Aerospace Engineering*, Vol. 221, Issue 1, 2007, pp. 47-55.